

Capacity Bounds on the Ergodic Capacity of Distributed MIMO Systems over \mathcal{K} Fading Channels

XingWang Li¹, Junfeng Wang¹, Lihua Li² and Charles C. Cavalcante³

¹School of Physics and Electronic Information Engineering, Henan Polytechnic University
No.2001, Century Avenue, Jiaozuo, China

[e-mail:lixingwangbupt@gmail.com, wangjunfeng@hpu.edu.cn]

²The State Key Laboratory of Networking and Switching Technology, Beijing University of Posts and
Telecommunication No.10, Xitucheng Road, Haidian District, Beijing, China

[e-mail: lilihua@bupt.edu.cn]

³Wireless Telecommunications Research Group, Federal University of Ceará,
Campus do Pici, Bl. 722, ZIP 60455-760, Fortaleza-CE, Brazil

[e-mail: charles@gtel.ufc.br]

*Corresponding author: Lihua Li

Received April 15, 2016; accepted May 31, 2016; published July 31, 2016

Abstract

The performance of D-MIMO systems is not only affected by multipath fading but also from shadowing fading, as well as path loss. In this paper, we investigate the ergodic capacity of D-MIMO systems operating in non-correlated \mathcal{K} fading (Rayleigh/Gamma) channels. With the aid of majorization and Minkowski theory, we derive analytical closed-form expressions of the upper and lower bounds on the ergodic capacity for D-MIMO systems over non-correlated \mathcal{K} fading channels, which are quite general and applicable for arbitrary signal-to-noise ratio (SNR) and the number of transceiver antennas. To intuitively reveal the impacts of system and fading parameters on the ergodic capacity, we deduce asymptotic approximations in the high and low SNR regimes. Finally, we pursue the massive MIMO systems analysis for the lower bound and derive closed-form expressions when the number of antennas at BS grows large, and when the number of antennas at transceivers becomes large with a fixed and finite ratio. It is demonstrated that the proposed expressions on the ergodic capacity accurately match with the theoretical analysis.

Keywords: D-MIMO, \mathcal{K} fading channel, majorization theory, ergodic capacity

This work was supported by the National Science and Technology Major Project (no. 2015ZX03001034), the Doctoral Scientific Funds of Henan polytechnic University (no. B2016-34), the National Natural Science Foundation of China (Grant no. 61501404), the Open Research Fund of State Key Laboratory of Networking and Switching Technology of Beijing University of Posts and Telecommunications (no. SKLNST-2016-1-02).

1. Introduction

Recently, distributed multiple-input multiple-out (D-MIMO) wireless communication systems have received significant attention as they can combine the advantages of point-to-point MIMO with distributed antenna system (DAS) [1]-[4]. These gains are achieved by deploying multiple antennas at the radio ports (RPs) that are geographically distributed. Contrary to collocated MIMO (C-MIMO) system, D-MIMO system suffers from different degrees of shadowing fading and path losses caused by different geographical positions and access distances. This makes the performance analysis of D-MIMO systems more challenging. However, large-scale fading (shadowing fading and path loss) is a crucial factor to assess the performance of D-MIMO systems [5][6]. For this reason, we herein investigate the capacity of D-MIMO systems over composite fading channels.

In the context of composite fading channels, Rayleigh/Lognormal (RLN) model is known as the most prevalent model, which has been extensively used to characterize the effects of composite fading in terrestrial and satellite wireless communication [7]-[11]. The main drawback of the RLN model is that the probability density function (PDF) of the composite fading model involves complicated mathematical formulas, which renders them inconvenient for analytical performance evaluations. To solve this issue, the friendlier Gamma distribution was used to approximate the lognormal distribution leading to the \mathcal{K} composite distribution model (Rayleigh/Gamma distribution) [12]. Some empirical measurements reveal a general consensus that \mathcal{K} fading model can capture diverse scattering phenomena such as tropospheric propagation of radio waves [5][13], various types of radar clutter [14], and optical scintillation from the atmosphere [15].

Motivated by the previous discussion, a plethora of recent works focus on the performance of \mathcal{K} fading MIMO systems. In [16], authors investigate the outage probability performance of correlated- \mathcal{K} fading channels with arbitrary and not necessarily identical parameters, while [17] provides the exact expressions on outage probability for exponentially correlated \mathcal{K} fading channels. Finally, [18][18] consider the performance of correlated \mathcal{K} fading MIMO channels with zero-forcing (ZF) receivers. To the best of authors' knowledge, there is no work about ergodic capacity bounds of D-MIMO systems over spatially non-correlated \mathcal{K} fading channels. In this light, we herein try to bridge this gap by presenting the upper and lower bounds on the ergodic capacity for spatially non-correlated \mathcal{K} fading channel. In particular, the main contributions of this paper are summarized as follows:

(1) The analytical upper and lower bounds of ergodic capacity for spatially non-correlated \mathcal{K} fading channel are derived by virtue of majorization and Minkowski theory. The proposed upper bound can be obtained by investigating the relationships between eigenvalues and diagonal elements of the Wishart matrix. The proposed lower bound can be obtained with the aid of the Minkowski's inequality.

(2) In order to reveal intuitive insights into the impacts of system parameters on the ergodic capacity, we pursue the asymptotic analysis in the low and high signal-to-noise ratio (SNR) regimes. In the low SNR regime, we explore the asymptotic performance by two metrics of the minimum normalized energy per information bit to reliably convey any positive rate and the wideband slope. In the high SNR regime, the effects of small and large-scale fading on the ergodic capacity are decoupled.

(3) Based on the proposed lower bound, we explore the asymptotic system performance for the massive MIMO system by deploying a large number of antennas at the BS and at both

ends with a fixed and finite ratio. It is demonstrated that the effect of small-scale fading is canceled and the sum rate is affected by the large-scale shadowing fading and path loss.

The remainder of the paper is organized as follows: In Section 2, we introduce the D-MMO fading model and provide the definition of ergodic capacity. In Section 3, some mathematical preliminaries are provided for analysis. In Section 4, we derive closed-form upper and lower bounds on the ergodic capacity of the spatially non-correlated \mathcal{K} fading channel and perform the asymptotic analysis in the low and high SNR regimes and massive MIMO systems. Some numerical results and corresponding analysis are presented in Section 5. Section 6 concludes the paper and summarizes the key findings.

Notation: Upper and lower case boldfaces are denoted the matrix and vector, respectively, while the notations \mathbb{C} and \mathbb{R} denote the sets of complex and integer numbers, respectively. Let \cdot^T , \cdot^H , \cdot^{-1} and \cdot^\dagger denote transpose, conjugate transpose, inverse, and pseudoinverse operations of a matrix, respectively. The notation \mathbf{I}_p denotes $p \times p$ the identity matrix. The notation $\mathcal{E} \cdot$ stands for the expectation operation, while the notation \prec denotes the majorization relation. The notation \cdot_{ij} denotes the i, j -th entry of a matrix and $\det \cdot$ stands for the determinant of a square matrix. Finally, the notations $\mathbf{d} \cdot$ and $\lambda \cdot$ represent the main diagonal elements and eigenvalues of a Hermitian matrix, respectively.

2. D-MIMO Fading Model and Ergodic Capacity

2.1 D-MIMO Fading Model

We consider a general uplink D-MIMO system with one base station (BS) connected with N_r receive antennas and L radio ports (RPs) each connected with N_t transmit antennas. As in [2][5][10][11], no channel state information (CSI) is assumed at the RPs, and full CSI is assumed at the BS. The optimum transmission strategy is that the total power is equally split by the LN_t antennas. Thus, the corresponding input-output relation is

$$\mathbf{y} = \sqrt{\frac{P}{LN_t}} \mathbf{H} \mathbf{\Xi}^{1/2} \mathbf{x} + \mathbf{n} \quad (1)$$

where $\mathbf{y} \in \mathbb{C}^{N_r \times 1}$ and $\mathbf{x} \in \mathbb{C}^{LN_t \times 1}$ are the received and transmitted signal vector, respectively, whereas $\mathbf{n} \in \mathbb{C}^{N_r \times 1}$ is the additive white Gaussian noise (AWGN) with zero mean and covariance $\mathcal{E}[\mathbf{n}\mathbf{n}^H] = N_0 \mathbf{I}_{N_r}$, where N_0 is the noise power.

The random matrix $\mathbf{H} \in \mathbb{C}^{N_r \times LN_t}$ captures small-scale fading, whose elements are modeled as independent and identically distributed (i.i.d.) $\mathcal{CN}(0,1)$ random variables (RVs). Therefore, the envelope of $r = |h_{ij}|$ follows a Rayleigh distribution [19]

$$p(r) = \frac{2r}{\Omega} \exp\left(-\frac{r^2}{\Omega}\right) U(r) \quad (2)$$

where $\Omega = \mathcal{E}[r^2]$ is the average power, and $U(r)$ is the unit step function. In our case, the value of the parameter Ω is assumed to be equal to unity.

The diagonal matrix $\mathbf{\Xi} \in \mathbb{R}^{LN_t \times LN_t}$ captures large-scale fading, which includes shadowing fading and path loss. It can be expressed as

$$\Xi = \text{diag} \left\{ \xi_m / D_m^v \mathbf{I}_{N_t} \right\}_{m=1}^L \tag{3}$$

where D_m denotes the distance between BS and the m -th RP, $m = 1, \dots, L$, $v \in 2, 5$ is the path loss exponent, which is a key metric to characterize the rate of decay of the signal with the distance [20]. The shadowing fading is captured by coefficient ξ_m , which is modeled as a Gamma RV. In this case, the PDF of coefficient ξ_m is given as

$$p_{\xi_m}(\xi_m) = \frac{\xi_m^{k_m-1}}{\Gamma(k_m) \Omega_m^{k_m}} \exp\left(-\frac{\xi_m}{\Omega_m}\right), \xi_m, \Omega_m, k_m \geq 0 \tag{4}$$

where k_m and $\Omega_m = \mathcal{E} \xi_m / k_m$ represent the shape and scale parameters of the Gamma distribution respectively, whereas $\Gamma(\cdot)$ is the Gamma function as defined in [21].

2.2 Ergodic Capacity

As stated previously, we consider that BS has perfect knowledge of CSI, and an equal-power allocation strategy across all the RP's antennas is executed. Then, the ergodic capacity of the D-MIMO systems is given as [5]

$$C = \mathcal{E} \left[\log_2 \left(\det \left(\mathbf{I} + \frac{\gamma}{LN_t} \mathbf{W} \right) \right) \right] \tag{5}$$

where $\gamma = P/N_0$ is the average SNR, $\mathbf{W} = \Xi^{1/2} \mathbf{H}^H \mathbf{H} \Xi^{1/2}$ and the expectation operation is taken over all random matrices \mathbf{H} and Ξ (or likewise \mathbf{W}). For the Hermitian matrix \mathbf{W} , we define that

$$\mathbf{W} = \begin{cases} \mathbf{H} \Xi \mathbf{H}^H & N_r \leq LN_t \\ \Xi^{1/2} \mathbf{H}^H \mathbf{H} \Xi^{1/2} & N_r > LN_t \end{cases} \tag{6}$$

In this correspondence, we focus on the case $N_r > LN_t$. All the results can be extended to the case of $N_r \leq LN_t$ by employing the identity

$$\det \left(I_{LN_t} + \frac{\gamma}{LN_t} \Xi^{1/2} \mathbf{H}^H \mathbf{H} \Xi^{1/2} \right) = \det \left(I_{N_r} + \frac{\gamma}{LN_t} \mathbf{H} \Xi \mathbf{H}^H \right) \tag{7}$$

By using the singular value decomposition, the ergodic capacity in (5) can be re-written as

$$C = \mathcal{E} \left[\sum_{m=1}^{LN_t} \log_2 \left(1 + \frac{\gamma}{LN_t} \lambda_m \right) \right] \tag{8}$$

where λ_m is the m -th eigenvalue of the Hermitian matrix \mathbf{W} .

3. Mathematical Preliminaries

In this section, RV distribution properties and majorization theory are presented to execute the bounds analysis for non-correlated \mathcal{K} fading D-MIMO system. These conclusions will be used in Section 4.

3.1 RV Distribution

Lemma 1: [19] Let $X \sim \mathcal{R}(\Omega)$ be a Rayleigh RV. Then, the RV $Y = X^2$ follows an exponential distribution with mean Ω . That is, the PDF of Y is

$$p_Y(y) = \frac{1}{\Omega} \exp\left(-\frac{y}{\Omega}\right) U(y) \quad (9)$$

Lemma 2: [19] Let X_i , $i=1, \dots, n$ be a set of n i.i.d. exponential RVs with mean Ω . Then, the RV $Y = \sum_{i=1}^n X_i$ follows a Gamma distribution with the shape parameter n and scale parameter Ω . Then, the PDF of the RV Y is

$$\sum_{i=1}^n X_i \sim \mathcal{G}(n, \Omega) \quad (10)$$

Lemma 3: [19] Let X_i , $i=1, \dots, n$ be a set of n independent Gamma RV with the same scale parameter Ω but possibly different shape parameters μ_1, \dots, μ_n , respective. Then

$$\sum_{i=1}^n X_i \sim \mathcal{G}\left(\sum_{i=1}^n \mu_i, \Omega\right) \quad (11)$$

3.2 Majorization Theory

Majorization theory is an extremely useful and powerful tool for the theory of inequalities [22] and recently has been extensively used in wireless communication field [23]. The relevant results of majorization theory are provided for our analysis.

Lemma 4: [22][23] Let \mathbf{R} be a Hermitian matrix with diagonal elements denoted by the vector \mathbf{d} and eigenvalues denoted by the vector $\boldsymbol{\lambda}$. Then

$$\boldsymbol{\lambda} \prec \mathbf{d} \quad (12)$$

Lemma 5: [22][23] Let ϕ be the real-valued function on \mathbb{R}^n . If $g: \mathbb{R} \rightarrow \mathbb{R}$ is concave. Then ϕ , which is defined as

$$\phi = \sum_{i=1}^n g(x_i) \quad (13)$$

is Schur-concave. In the same way, if g is convex, then ϕ is Schur-convex.

Lemma 6: [25][26] Let ϕ be the real-valued function on \mathbb{R}^n , which is defined as

$$\phi = \sum_{i=1}^n \log_2(1 + \alpha x_i), \alpha > 0 \quad (14)$$

Then, ϕ is a Schur-concave function.

4. Ergodic Capacity Bounds for D-MIMO Systems

In this section, we elaborate on the ergodic capacity of spatially non-correlated \mathcal{K} fading D-MIMO systems, where multipath, shadowing fading and path loss are considered. In view of majorization [22]-[26] and Minkowski theory [27][28], the analytical upper and lower bounds on the ergodic capacity of D-MIMO systems are derived. In order to obtain the insightful insights into the impacts of the system parameters on the ergodic capacity, the asymptotic approximations on the ergodic capacity at high and low SNR regimes are provided.

4.1 Ergodic Capacity Upper Bound

Using the results of [25], we provide a novel upper bound of the ergodic capacity for non-correlated \mathcal{K} fading channels. The result will be given in the following theorem.

Theorem 1: For non-correlated \mathcal{K} fading channels, the upper bound of the ergodic capacity for D-MIMO systems is gives as

$$\bar{C} = \frac{N_t}{\ln 2 \Gamma} \sum_{m=1}^L \frac{1}{N_r \Gamma} \frac{1}{k_m} G_{42}^{14} \left[\frac{\gamma \Omega_m}{LN_t D_m^v} \middle| \begin{matrix} 1-k_m, 1-N_r, 1, 1 \\ 1, 0 \end{matrix} \right] \quad (15)$$

where $G \cdot$ is the Meijer’s G function as defined in [21].

Proof: A detail proof is provided Appendix I. ■

It is noteworthy that the proposed upper bound involves Meijer’s G-function which can be efficiently evaluated by standard mathematical software packages like Mathematica or Maple. Moreover, the formula (15) reduces to the result of [25, Th. 1] under the case of $L=1$ and $\Xi = \mathbf{I}_{N_t}$.

Although the formula in (15) presents a closed-form analytical expression, it does not give useful insights into the impacts of systems parameters on the ergodic capacity. In this light, we perform the asymptotic analysis in the high and low SNR regimes.

Corollary 1: For high SNR regime, the upper bound in (15) becomes

$$\bar{C}^H = LN_t \log_2 \left(\frac{\gamma}{LN_t} \right) + LN_t \frac{\varphi N_r}{\ln 2} + N_t \sum_{m=1}^L \left[\frac{\varphi k_m}{\ln 2} + \log_2 \Omega_m - v \log_2 D_m \right] \quad (16)$$

where $\varphi \cdot = d \ln \Gamma \cdot / dx$ is the digamma function as defined in [21].

Proof: In high SNR (large γ), the dominant term of logarithmic function is $\gamma \chi_m / LN_t D_m^v$. Thus, the function $\log_2 (1 + \gamma \chi_m / LN_t D_m^v)$ can be approximated by $\log_2 \gamma \chi_m / LN_t D_m^v$. In turn, we use the following integral identities [21].

$$\int_0^\infty x^{v-1} \exp -\mu x \ln x dx = \frac{\Gamma v}{\mu^v} [\varphi v - \ln \mu], \text{Re } \mu, v > 0 \quad (17)$$

$$\int_0^\infty x^{v-1} \exp -\mu x dx = \frac{\Gamma v}{\mu^v}, \text{Re } \mu, v > 0 \quad (18)$$

After some simplification, we complete the proof. ■

The above corollary reveals that the effects of large- and small-scale fading can be decoupled for high SNRs. The similar result appears in [2]. Moreover, we can observe that the proposed upper bound increases logarithmically with transmit power γ . More important, N_r, k_m and Ω_m have a beneficial impact on the upper bound where a large transceivers distance D_m effectively reduces it since large distance yields large path loss.

In general, it is straightforward to study low SNR performance by deriving the first-order Taylor expansion of the proposed upper bound around $\gamma \rightarrow 0$. The recent publications, e.g., [29][30] have shown that this approach can not adequately reflect the impact of the system parameters on D-MIMO performance and lead to misleading results in the low-SNR regime. In this light, it is beneficial to analyze the upper bound at low SNR regime in terms of the normalized transmit energy per information bit E_b/N_0 rather than SNR, which is originally proposed in [29]. Hence, the upper bound at low-SNRs is formulated as

$$\bar{C}^L \left(\frac{E_b}{N_0} \right) \approx \mathcal{S}_0 \log_2 \left(\frac{\frac{E_b}{N_0}}{N_{0 \min}} \right) \quad (19)$$

$$\frac{E_b}{N_{0 \min}} = \frac{1}{\bar{C}'(0)}, S_0 = -\frac{2}{\log_2 e} \frac{\bar{C}''(0)}{\bar{C}'(0)^2} \quad (20)$$

where $E_b/N_{0 \min}$ is minimum normalized energy per information bit required to convey any non-negative rate reliably, while S_0 is the capacity versus SNR slope. $\bar{C}'(0)$ and $\bar{C}''(0)$ are the first and second derivatives of the proposed upper bound.

Corollary 2: For low SNR, the metrics of the minimum energy per information bit and the wideband slope are given respectively

$$\frac{E_b}{N_{0 \min}} = \frac{L \ln 2}{N_r} \left(\sum_{m=1}^L \frac{k_m \Omega_m}{D_m^v} \right)^{-1} \quad (21)$$

$$S_0 = \frac{2N_r N_t}{N_r + 1} \frac{\left(\sum_{m=1}^L \frac{k_m \Omega_m}{D_m^v} \right)^2}{\sum_{m=1}^L \frac{\Omega_m^2 k_m (k_m + 1)}{D_m^{2v}}} \quad (22)$$

Proof: The proof starts by rewrite (49)

$$\bar{C} = \frac{1}{\ln 2} \sum_{m=1}^{LN_t} \mathcal{E} \left[\ln \left(1 + \frac{\gamma}{LN_t D_m^v} \zeta \xi_m \right) \right] \quad (23)$$

By taking the first and second derivatives of (23) with respect to $\gamma \rightarrow 0$. We can derive as

$$\begin{aligned} \bar{C}'(0) &= \frac{1}{\ln 2} \sum_{m=1}^{LN_t} \mathcal{E} \left[\frac{\frac{\zeta \xi_m}{LN_t D_m^v}}{1 + \frac{\gamma}{LN_t D_m^v} \zeta \xi_m} \right]_{\gamma=0} \\ &= \frac{1}{LN_t \ln 2} \sum_{m=1}^{LN_t} \mathcal{E} \left[\frac{\zeta \xi_m}{D_m^v} \right] \end{aligned} \quad (24)$$

$$\begin{aligned} \bar{C}''(0) &= \frac{-1}{\ln 2} \sum_{m=1}^{LN_t} \mathcal{E} \left[\frac{\left(\frac{\zeta \xi_m}{LN_t D_m^v} \right)^2}{\left(1 + \frac{\gamma}{LN_t D_m^v} \zeta \xi_m \right)^2} \right]_{\gamma=0} \\ &= \frac{-1}{LN_t^2 \ln 2} \sum_{m=1}^{LN_t} \mathcal{E} \left[\frac{\zeta^2 \xi_m^2}{D_m^{2v}} \right] \end{aligned} \quad (25)$$

With the aid of the definition of expectation and successively applying (18), the formulas (24) and (25) can be further simplified as

$$\bar{C}'(0) = \frac{N_r}{LN_t \ln 2} \sum_{m=1}^{LN_t} \left(\frac{k_m \Omega_m}{D_m^v} \right) \quad (26)$$

$$\bar{C}''(0) = -\frac{N_r N_r + 1}{LN_t^2 \ln 2} \sum_{m=1}^{LN_t} \left(\frac{\Omega_m^2 k_m (k_m + 1)}{D_m^{2v}} \right) \quad (27)$$

Finally, the result of (21) and (22) can be derived by substituting (26) and (27) into (20). After some manipulations, the proof of the proposition is completed. ■

The proposition reveals that the result of (21) is determined by the number of receiver antennas N_r , the number of RP L , shadowing fading parameters k_m and Ω_m , and path loss parameter d_m and v , while the result is independent of the number of RP's antenna N_t . Note that the similar results have been appeared in [31]. For $\Xi = \mathbf{I}_{LN_t}$, $L = 1$, the two metrics reduce to $E_b/N_{0\min} = L \ln 2/N_r$ and $\mathcal{S}_0 = 2N_r N_t / N_r + 1$, which is consistent with [18][31].

4.2 Ergodic Capacity Lower Bound

In this subsection, we derive an analytical lower bound expression on the ergodic capacity of D-MIMO system over non-correlated \mathcal{K} fading channel. The key result is summarized in the following theorem.

Theorem 2: For non-correlated \mathcal{K} fading D-MIMO channels, the lower bound of the ergodic capacity for D-MIMO systems is

$$\underline{C} = LN_t \log_2 \left(1 + \frac{\gamma}{LN_t} \exp \left(\frac{1}{LN_t} \sum_{m=0}^{LN_t-1} \varphi N_r - m + \frac{1}{L} \sum_{m=1}^L \varphi k_m + \ln \Omega_m - v \ln D_m \right) \right) \quad (28)$$

Proof: The proof is provided in Appendix II. ■

It is observed that the lower bound of the ergodic capacity monotonically increases with the number of BS antenna N_r , the fading parameter k_m and the transmit power γ while decreases with the transceiver distances D_m . In addition, there are similarities between (28) and (16). Finally, the similar conclusions are also made in [10].

In order to obtain the intuitive insights into the impact of systems parameter, the asymptotic performance at high SNR regime is examined in the following proposition

Corollary 3: For high SNR, the lower bound in (28) converges to

$$\underline{C}^H = LN_t \log_2 \left(\frac{\gamma}{LN_t} \right) + \frac{1}{\ln 2} \sum_{m=0}^{LN_t-1} \varphi N_r - m + N_t \sum_{m=1}^L \left(\frac{\varphi k_m}{\ln 2} + \log_2 \Omega_m - v \log_2 D_m \right) \quad (29)$$

Proof: After some simplification, we can complete the proof by taking transmit power γ large ($\gamma \rightarrow \infty$). ■

Comparing Proposition 1 and Proposition 3, we can conclude that the two propositions have the similar conclusion except the small-scale fading. Moreover, (16) and (28) converge the same result for large antennas systems by using the property of digamma function.

In order to obtain the diversity order of the D-MIMO system, the expression on the lower bound of ergodic capacity is studied at high SNR. In this corresponding, we execute the analysis by invoking the affine expansion of the lower bound of the ergodic capacity [11]

$$\underline{C}^\infty = \mathcal{S}_\infty \log_2 \gamma - \mathcal{L}_\infty + o(1) \quad (30)$$

where \mathcal{S}_∞ and \mathcal{L}_∞ represent the high-SNR slope in bits/s/Hz per 3-dB units and the high-SNR power offset, in 3-dB units, respectively, which are formulated as

$$\mathcal{S}_\infty = \lim_{\gamma \rightarrow \infty} \frac{\underline{C}^\infty}{\log_2 \gamma} \quad (31)$$

$$\mathcal{L}_\infty = \lim_{\gamma \rightarrow \infty} \left(\log_2 \gamma - \frac{\underline{C}^\infty}{\mathcal{S}_\infty} \right) \quad (32)$$

Corollary 4: For high SNR, the metrics of the high-SNR slope and high-SNR power offset are provided

$$\mathcal{S}_\infty = LN_t \quad (33)$$

$$\mathcal{L}_\infty = \log_2 LN_t - \frac{1}{LN_t \ln 2} \sum_{m=0}^{LN_t-1} \varphi N_r - m - \frac{1}{L} \sum_{m=1}^L \left(\frac{\varphi k_m}{\ln 2} + \log_2 \Omega_m - v \log_2 D_m \right) \quad (34)$$

Proof: The process of the proof references proposition 2 of [11]. Omitting explicit details, we complete the proof. ■

It is intuitively observed that high-SNR slope \mathcal{S}_∞ in (34) is independent of the BS antenna number N_r , shadowing fading parameters k_m and Ω_m , and path loss parameters D_m and v . The similar observation is appeared in [11]. For high-SNR power offset \mathcal{L}_∞ , the effects of the large and small-scale can be decoupled. Finally, the larger distances between BS and RPs D_m , the much more effectively reduce the system performance due to the increased path loss.

4.3 Massive MIMO Analysis

Recently, massive MIMO has emerged as one of the most promising technologies since it has the potential to improvement spectral and energy efficiency [32]-[34]. In the following, we study the asymptotic performance of massive MIMO system for the lower bound of theorem 2.

In order to obtain the intuitive insights into the massive MIMO analysis, the three separate cases are considered:

(1) Fixed L and N_t , whilst $N_r \rightarrow \infty$: Directly, when the number of the BS antennas grows without bound, whilst L and N_t are kept fixed, the ergodic capacity lower bound of (28) tends to infinity.

Corollary 5: Fixed L and N_t , while $N_r \rightarrow \infty$, the lower bound of the ergodic capacity becomes

$$\underline{C} = LN_t \log_2 \left(1 + \frac{\gamma N_r}{LN_t} \exp \left(\frac{1}{L} \left(\sum_{m=1}^L \varphi k_m + \ln \Omega_m - v \ln D_m \right) \right) \right) \quad (35)$$

Proof: The proof starts by introducing the follow identity [35]

$$\varphi x \approx \ln x \quad x \rightarrow \infty \quad (36)$$

Substituting (36) into (28), we can obtain the desired result of (36) after some simplifications. ■

From the result of (35), we can observe that the effects of small-scale fading can be omitted for the number of the BS antennas grows without bound. The similar appears in [2]. Moreover, the ergodic capacity grows into infinity with BS antennas.

(2) Fixed $L, \kappa = N_r/LN_t > 1$, whilst $N_t, N_r \rightarrow \infty$: In this case, the number of the BS and each user's antennas grows large with a fixed and finite ratio, whilst the number of users is kept fixed.

Corollary 6: Fixed L, κ , whilst $N_t, N_r \rightarrow \infty$, the lower bound of the ergodic capacity becomes

$$\underline{C} = LN_t \log_2 \left(1 + \frac{\gamma \kappa^\kappa}{\exp 1 \kappa - 1} \exp \left(\frac{1}{L} \left(\sum_{m=1}^L \varphi k_m + \ln \Omega_m - v \ln D_m \right) \right) \right) \quad (37)$$

Proof: The proof starts by re-writing (29) as follows

$$\underline{C} = LN_t \log_2 \left(1 + \frac{\gamma}{LN_t} \exp \left(\frac{1}{LN_t} \sum_{m=0}^{LN_t-1} \varphi N_r - m + \frac{1}{LN_t} \left(\sum_{m=1}^{LN_t} \varphi k_m + \ln \Omega_m - v \ln D_m \right) \right) \right) \quad (38)$$

By using (36), the first sum term in (38) can be expressed as

$$\frac{1}{LN_r} \sum_{m=0}^{LN_r-1} \varphi N_r - m \approx \ln N_r + \frac{1}{LN_r} \sum_{m=0}^{LN_r-1} \ln \left(1 - \frac{m}{N_r} \right) \quad (39)$$

The second sum term in (39) can be written as in integral form

$$\frac{1}{LN_r} \sum_{m=0}^{LN_r-1} \ln \left(1 - \frac{m}{N_r} \right) = \frac{1}{LN_r} \int_0^{LN_r} \ln \left(1 - \frac{m}{N_r} \right) dm \quad (40)$$

Recalling the following integral identity [36]

$$\int_0^m \ln \left(1 - \frac{x}{n} \right) dx = m - n \ln \left(1 - \frac{m}{n} \right) - m, \quad n > m \quad (41)$$

Combining (39), (40), (41) with (38), we can conclude the proof after some algebraic manipulations. ■

Through corollary 6, we can conclude that the ergodic capacity linear increases with transmit antennas and logarithmically increases with transmit power γ .

(3) Fixed $N_r, \kappa = N_r/LN_r > 1$, whilst $L, N_r \rightarrow \infty$: In this case, it is equivalent that all users are mutually independent and uniformly distributed in the circle of the cell. It is assumed that the shadow fading parameters are fixed constant, i.e., $k_m = k$, $\Omega_m = \Omega_0$. Thus, the PDF of the distance between the BS and users is given by [37]

$$p_D(x) = \frac{2x}{R_0^2 - r_0^2}, \quad r_0 \leq x \leq R_0 \quad (42)$$

Corollary 7: Fixed N_r, κ , whilst $L, N_r \rightarrow \infty$, the lower bound of the ergodic capacity becomes

$$\underline{C} = LN_r \log_2 \left(1 + a \exp \left(v \left(\frac{1}{2} - \frac{R_0^2 \ln R_0 - r_0^2 \ln r_0}{R_0^2 - r_0^2} \right) \right) \right) \quad (43)$$

where $a = \gamma \Omega_0 \kappa^\kappa \kappa - 1^{1-\kappa} \exp \varphi k - 1$, R_0 is the radius of the cell, r_0 is the closest distance between the users and BS.

Proof: Using the shadow fading parameter assumption, the lower bound of corollary 6 can be further simplified as

$$\underline{C} = LN_r \log_2 \left(1 + \gamma \Omega_0 \kappa^\kappa \kappa - 1^{1-\kappa} \exp \varphi k - 1 \exp \left(\frac{1}{L} \left(\sum_{m=1}^L \underbrace{-v \ln D_m}_{\textcircled{1}} \right) \right) \right) \quad (44)$$

By using the relation between the sum and expectation, the sum term in (44) is expressed in integral form

$$\textcircled{1} = \mathcal{E}[-v \ln D_m] \quad (45)$$

Based on the definition of expectation and the PDF of D_m in (42), $\textcircled{1}$ can be further expressed as

$$\textcircled{1} = \frac{-2v}{R_0^2 - r_0^2} \int_{r_0}^{R_0} D_m \ln D_m dD_m \quad (46)$$

We now recall the following integral identity [36]

$$\int_m^n x \ln x dx = \frac{n^2 \ln n - m^2 \ln m}{2} - \frac{n^2 - m^2}{4}, \quad n > m > 0 \quad (47)$$

Substituting (47) into (44), we can conclude the proof after some manipulations. ■

Corollary 7 reveals that the result of (43) is quite general, which can be applied to arbitrary number of the transceiver antennas. Moreover, it is inferred that a large value R_0 reduces the ergodic capacity while a large value r_0 increases it.

5. Numerical Results

In this section, some numerical results are presented to further validate the derived analytical results. For all simulations, it is assumed that there are $L = 3$, $N_t = 2$ except Fig. 3. We reape the multipath and shadowing fading matrix \mathbf{H} and $\mathbf{\Xi}$ according (2) and (4) by generating 100000 random realizations and thereafter get the simulated ergodic capacity via (5).

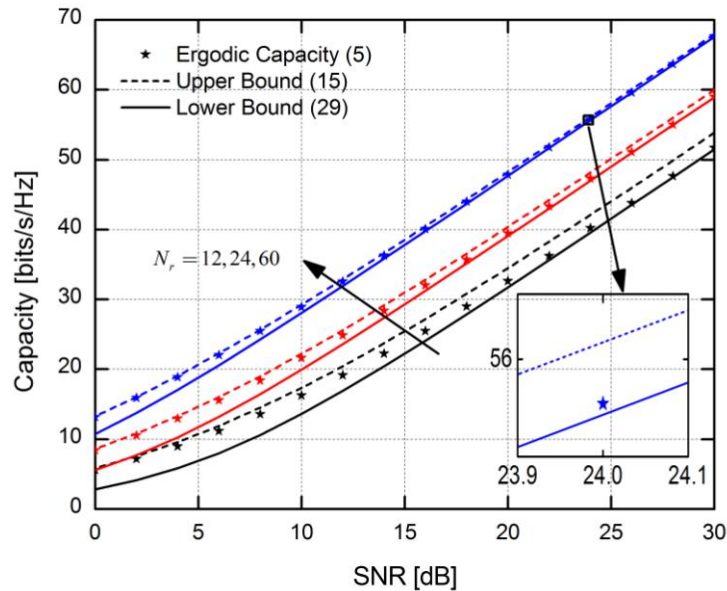


Fig. 1. Simulated ergodic capacity, analytical upper and lower bounds versus the SNR ($L = 3$, $N_t = 2$, $\Omega = 1$, $k_m = 1$, $\Omega_m = 2$, $v = 4$, $D_1 = 1000m$, $D_2 = 1500m$, $D_3 = 2000m$)

In Fig. 1, the tightness of the analytical upper bound in (15) and lower bound in (29) are investigated. In this simulation settings, we assume that $N_r = 12, 24, 60$, $N_t = 2$, $L = 3$, $\Omega = 1$, $k_m = 1$, $\Omega_m = 2$, $v = 4$, $D_1 = 1000m$, $D_2 = 1500m$, $D_3 = 2000m$, $L = 1, \dots, L$. We first get the simulated ergodic capacity via (5).

Clearly, the proposed upper and lower bounds tighten when the large number of BS antennas grows large. The upper bound matches the simulated ergodic capacity across the entire SNRs, while the lower bound converges to the exact high-SNR ergodic capacity, which is consistent with [18][38]. Then, we also observe that the lower bound is tighter than the upper bound for the high SNR regime. For $N_r = 60$, the curves of the upper bound and the simulated result are almost coincidence. For the high SNR regime, the curves of the lower bound and the simulated result are almost overlapped.

In Fig. 2, the asymptotic high SNR approximations for the upper bound in (16) and lower bound in (29) are compared with the simulated ergodic capacity in (5). The simulation

parameters are the same of Fig. 1. As anticipated, the proposed bounds remains relatively tight for high SNR regime and large number of BS antennas N_r . From the zoomed figure, we can also observe that the lower bound is tighter than the upper bound at high SNRs. Fig. 2 also reveals that the proposed bounds approach the Monte-Carlo simulation for large value N_r .

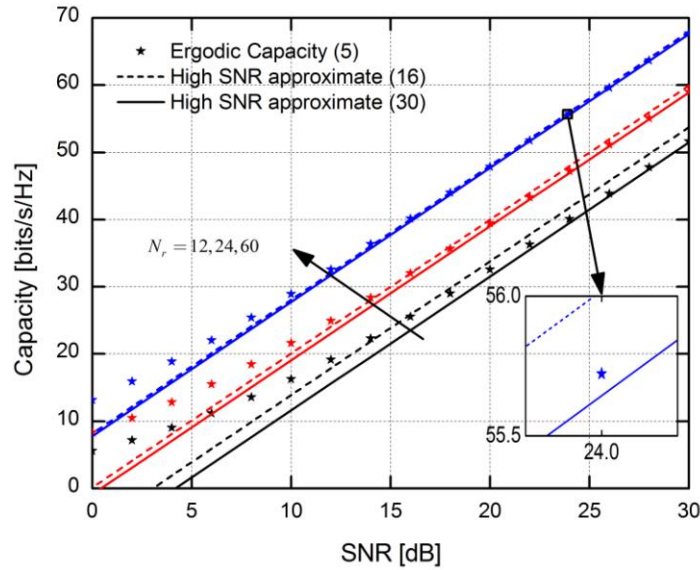


Fig. 2. Simulated ergodic capacity and high SNR approximations for upper and lower bounds versus SNR ($L=3, N_t=2, \Omega=1, k_m=1, \Omega_m=2, v=4, D_1=1000m, D_2=1500m, D_3=2000m$)

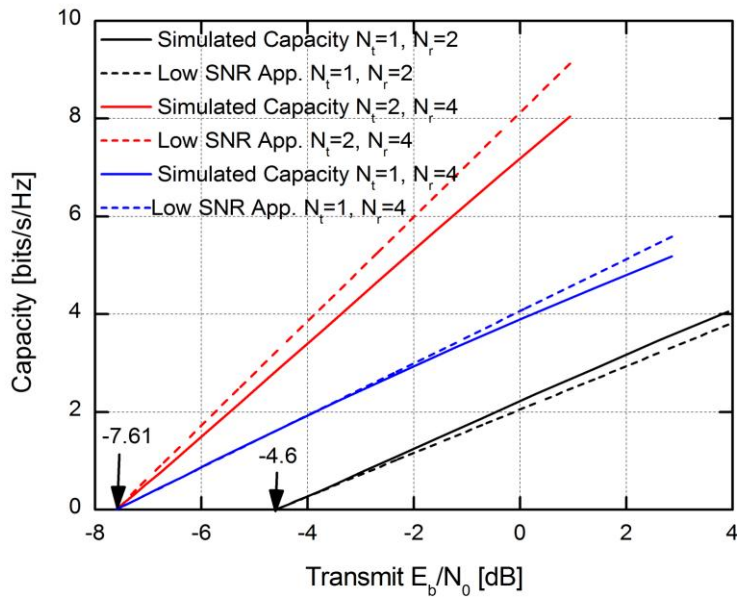


Fig. 3. Low SNR capacity versus transmit E_b/N_0 for different transceiver antennas ($N_t=1, N_r=2; N_t=2, N_r=2; N_t=1, N_r=4$)

In **Fig. 3**, we investigate the simulated ergodic capacity and low SNR approximate capacity in (19) versus transmit energy per bit E_b/N_0 (Proposition 2) for different transmit and receive antennas. For illustration purposes, we assume that the large scale fading matrix is set to the identity matrix $\Xi = \mathbf{I}_{LN_t}$ and $L = 1$. The **Fig. 3** reveals that increasing the number of receive antennas N_r reduces the required $E_b/N_{0\min}$, and the same number of receive antennas N_r has the same required $E_b/N_{0\min}$. These confirm the analysis of Proposition 2 and coincide with the results of [31]. Moreover, the figure shows the larger wideband slope \mathcal{S}_0 is obtained with higher N_r and N_t . Finally, we can also observe that the analytical results sufficiently match the simulated results at low SNR regime.

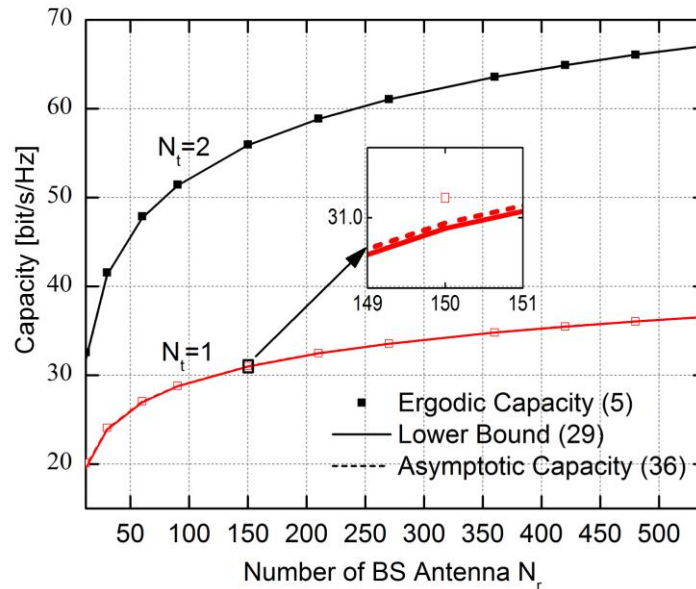


Fig. 4. Simulated ergodic capacity, lower bound and asymptotic capacity versus of the number of BS antennas ($P = 20\text{dB}$, $L = 3$, $\Omega = 1$, $k_m = 1$, $\Omega_m = 2$, $v = 4$, $D_1 = 1000\text{m}$, $D_2 = 1500\text{m}$, $D_3 = 2000\text{m}$)

The asymptotic capacity of large array systems is investigate in **Fig. 4** for the case of $N_t = 1$ and $N_t = 2$, respectively. It is readily observed that a larger N_t increases the diversity and multiplexing gains, thereby yielding a large capacity. In addition, the capacity grows logarithmically with the number of BS antennas N_r without bound. Finally, we can also observe that the curves of lower bound in (28) and asymptotic capacity in (35) almost overlap with the simulated ergodic capacity in (5).

6. Conclusion

In this paper, we elaborate on the ergodic capacity of D-MIMO systems over spatially non-correlated \mathcal{K} fading channels. In particular, the closed-form upper and lower bounds on ergodic capacity are derived with the aid of majorization and Minkowski theories. It is demonstrated that the proposed upper bound remains relatively tight across the entire SNR regime and when the number of BS and transceiver antennas grows large, while proposed

lower bound converges to the simulated results at high SNR regime. For high SNR regime, the lower bound is tighter than the upper bound, and vice versa. In order to obtain useful insights into the implications of the system parameters on the ergodic capacity, we also examine in detail the bounds of the asymptotic high and low SNR regimes. Finally, we explore the emerging area of massive MIMO systems in detail and the interesting results of the lower bound for the “large-systems” limits are derived. It is shown that the simulation results match theoretical analysis very well. The above analytical results encompass the Rayleigh multipath fading, Gamma shadowing fading and path loss of practical interest.

Appendix I: Proof of Theorem 1

Proof: The proof starts by rewriting the expression of ergodic capacity in (8)

$$C = \mathcal{E} \left[\sum_{m=1}^{LN_t} \log_2 \left(1 + \frac{\gamma}{LN_t} \lambda_m \right) \right] \quad (48)$$

Assuming that $\boldsymbol{\lambda} = \lambda_1, \dots, \lambda_{LN_t}$ is the eigenvalue vector of the Hermitian matrix \mathbf{W} in (6) and $\phi = \sum_{m=1}^{LN_t} \log_2 \left(1 + \frac{\gamma}{LN_t} \lambda_i \right)$. Applying Lemma 4, Lemma 5 and lemma 6, the ergodic capacity is upper bounded as

$$\bar{C} = \mathcal{E} \left[\sum_{m=1}^{LN_t} \log_2 \left(1 + \frac{\gamma}{LN_t} d_m \right) \right] \quad (49)$$

where $\mathbf{d} = d_1, \dots, d_{LN_t}$ is the diagonal of the Hermitian matrix \mathbf{W} in (6).

The expression on the upper bound of ergodic capacity can be further re-expressed as

$$\bar{C} = \sum_{m=1}^{LN_t} \mathcal{E} \left[\log_2 \left(1 + \frac{\gamma}{LN_t D_m^v} \chi_m \right) \right] \quad (50)$$

where p_{χ_m} is the PDF of d_m , while the RV χ_m , which includes multipath and shadowing fading, can be expressed as

$$\chi_m = \zeta_m \xi_m \quad (51)$$

where ξ_m is determined by formula (4), whereas the PDF of ζ_m , which is obtained by combining Lemma 1 with Lemma 2 and Lemma 3, is given as

$$p_{\zeta} = \frac{\zeta^{N_r-1}}{\Gamma(N_r)} \exp(-\zeta), \zeta \geq 0 \quad (52)$$

Now, the upper bound in (50) becomes

$$\bar{C} = \frac{1}{\ln 2} \sum_{m=1}^{LN_t} \mathcal{E} \left[\ln \left(1 + \frac{\gamma}{LN_t D_m^v} \zeta \xi_m \right) \right] \quad (53)$$

Then, the logarithmic function can be substituted by Meijer G function [39]

$$\ln(1+x) = G_{22}^{12} \left[x \begin{matrix} 1,1 \\ 1,0 \end{matrix} \right] \quad (54)$$

By using the definition of integral and the formula (55), the upper bound can be rewritten as

$$\bar{C} = \frac{1}{\ln 2} \sum_{m=1}^{LN_t} \int_0^\infty \int_0^\infty G_{22}^{12} \left[\frac{\gamma \zeta \xi_m}{LN_t D_m^v} \begin{matrix} 1,1 \\ 1,0 \end{matrix} \right] p_{\zeta}(\zeta) p_{\xi_m}(\xi_m) d_{\zeta} d_{\xi_m} \quad (55)$$

Finally, substituting (4) and (52) into (55) and successively applying the following integral

identity as [21]

$$\int_0^\infty x^{-\rho} \exp -\beta x G_{pq}^{mm} \left[\alpha x \begin{vmatrix} a_1, \dots, a_p \\ b_1, \dots, b_q \end{vmatrix} \right] dx = \beta^{\rho-1} G_{p+1,q}^{m,n+1} \left[\frac{\alpha}{\beta} \begin{vmatrix} \rho, a_1, \dots, a_p \\ b_1, \dots, b_q \end{vmatrix} \right] \quad (56)$$

We can complete the proof after some simple manipulation.

Appendix II: The proof of theorem 2

Proof: With the aid of the Minkowski's inequality [27][28], the ergodic capacity is lower bounded by

$$\underline{C} \geq LN_t \log_2 \left(1 + \frac{\gamma}{LN_t} \exp \left(\frac{1}{LN_t} \mathcal{E} [\ln \det \mathbf{W}] \right) \right) \quad (57)$$

By using the property of square matrices

$$\det \mathbf{AB} = \det \mathbf{A} \det \mathbf{B} \quad (58)$$

The lower bound in (58) can be further expressed as

$$\underline{C} = LN_t \log_2 \left(1 + \frac{\gamma}{LN_t} \exp \left(\frac{1}{LN_t} \underbrace{\mathcal{E} [\ln \det \mathbf{\Xi}]}_{\textcircled{1}} + \frac{1}{LN_t} \underbrace{\mathcal{E} [\ln \det \mathbf{H}^H \mathbf{H}]}_{\textcircled{2}} \right) \right) \quad (59)$$

Since large-scale matrix $\mathbf{\Xi}$ is diagonal, $\textcircled{1}$ in (59) can be formulized as

$$\begin{aligned} \textcircled{1} &= \mathcal{E} \left[\ln \left(\prod_{m=1}^{LN_t} \xi_m D_m^{-v} \right) \right] \\ &= \sum_{m=1}^{LN_t} \mathcal{E} [\ln \xi_m] - v \sum_{m=1}^{LN_t} \ln D_m \\ &\stackrel{a}{=} \sum_{m=1}^{LN_t} \varphi k_m + \ln \Omega_m - v \ln D_m \end{aligned} \quad (60)$$

where a stems from (17).

For $\textcircled{2}$, the desired result can be obtained in view of [35]

$$\mathcal{E} [\ln \det \mathbf{H}^H \mathbf{H}] = \sum_{m=1}^{LN_t-1} \varphi N_r - m \quad (61)$$

After some simplification, we can conclude the proof.

References

- [1] A. Sanderovich, S. Shamai, and Y. Steinberg, "Distributed MIMO Receiver-Achievable Rates and Upper bounds," *Trans. Inf. Theory*, vol. 55, no. 10, pp. 4419-4438, Oct. 2009. [Article \(CrossRef Link\)](#)
- [2] M. Matthaiou, C. Zhong, M. R. McKay, and T. Ratnarajah, "Sum Rate Analysis of ZF Receivers in Distributed MIMO Systems," *IEEE J. Sel. Areas Commun.*, vol. 31, no. 2, pp. 180-191, Feb. 2013. [Article \(CrossRef Link\)](#)
- [3] D. Wang, J. Wang, X. You, Y. Wang, M. Chen, and X. Hou, "Spectral Efficiency of Distributed MIMO Systems," *IEEE J. Sel. Areas Commun.*, vol. 31, no. 10, pp. 2112-2127, Oct. 2013. [Article \(CrossRef Link\)](#)
- [4] M. Dai, and C. W. Sung, "Achieving high diversity and multiplexing gains in the asynchronous parallel relay network," *Trans. Emerging Telecommun. Technol.*, vol. 24, no. 2, pp. 232-243, Feb. 2013. [Article \(CrossRef Link\)](#)

- [5] X. Li, L. Li, X. Su, Z. Wang, and P. Zhang, "Approximate Capacity Analysis of Distributed MIMO System over Generalized-K Fading Channels," in *Proc. of IEEE Wireless Commun. Netw. Conf. (WCNC)*, New Orleans, USA, pp. 235-240, Mar. 2015. [Article \(CrossRef Link\)](#).
- [6] M. Dai, S. Zhang, et al., "Network-Coded Relaying in Multi-user Multi-cast D2D Network," *Int. J. Antenna Propag.*, vol. 2014, ArticleID 58794, pp. 1-7, 2014. [Article \(CrossRef Link\)](#)
- [7] M. Dai, P. Wang, S. Zhang, B. Chen, H. Wang, X. Lin, and C. Sun, "Survey on Cooperative Strategies for Wireless Relay Channels," *Trans. Emerging Telecommun. Technol.*, vol. 25, no. 9, pp. 926-942, Sep. 2014. [Article \(CrossRef Link\)](#)
- [8] M. Dai, H. Wang, et al., "Opportunistic Relaying with Analog and Digital Network Coding for Two-Way Parallel Relay Channels," *IET Commun.*, vol. 8, no. 12, pp. 2200-2206, Aug. 2014. [Article \(CrossRef Link\)](#)
- [9] M. Dai, B. Mao, D. Shen, et al., "Incorporating D2D to Current Cellular Communication System," *Mobile Information Systems*, vol. 2016, no. 2732917, pp. 1-7, Mar. 2016. [Article \(CrossRef Link\)](#)
- [10] X. Li, L. Li, and L. Xie, "Achievable Sum Rate Analysis of ZF Receivers in 3D MIMO Systems," *KSII Trans. Int. Inf. Systems*, vol. 8, no. 4, pp. 1368-1389, 2014. [Article \(CrossRef Link\)](#)
- [11] F. Tan, H. Gao, X. Su, and T. Lv, "Sum Rate Analysis for 3D MIMO with ZF Receivers in Ricean/Lognormal Fading Channels," *KSII Trans. Int. Inf. Systems*, vol. 9, no. 7, pp. 2371-2388, Jun. 2015. [Article \(CrossRef Link\)](#)
- [12] A. Abdi, and M. Kaveh, "K Distribution: An Appropriate Substitute for Rayleigh-Lognormal Distribution in Fading Shadowing Wireless Channels," *Electron. Lett.*, vol. 34, Apr. 30, pp. 851-853, 1998. [Article \(CrossRef Link\)](#)
- [13] A. Abdi, H. A. Barger, and M. Kaveh, "A Simple Alternative to the Lognormal Model of Shadow Fading in Terrestrial and Satellite Channels," in *Proc. of IEEE Veh. Tech. Conf.(VTC)*, Oct. pp. 2058-2062, 2001. [Article \(CrossRef Link\)](#)
- [14] H. P. Wang, and K. Ouchi, "Accuracy of the K-Distribution Regression Model for Forest Biomass Estimation by High-Resolution Polarimetric SAR: Comparison of Model Estimation and Field Data," *IEEE Trans Geosci. Remote Sensing*, vol. 46, no. 4, pp. 1058-1064. 2008. [Article \(CrossRef Link\)](#)
- [15] K. Kiasaleh, "Performance of Coherent DPSK Free-Space Optical Communication Systems in K-Distributed Turbulence," *IEEE Trans. Commun.*, vol. 54, no. 4, pp. 604-607, 2006. [Article \(CrossRef Link\)](#)
- [16] P. S. Bithas, N. C. Sagias, P. T. Mathiopoulos, S. A. Kostopoulos, and A. M. Marsa, "On the correlated K-Distribution with Arbitrary Fading Parameters," *IEEE Signal Process. Lett.*, vol. 15, pp. 541-544, 2008. [Article \(CrossRef Link\)](#)
- [17] T. S. B. Reddy, R. Subadar, and P. R. Sahu, "Outage Probability of SC Receiver over Exponentially Correlated K Fading Channels," *IEEE Commun. Lett.*, vol. 14, no. 2, pp. 118-120, Feb. 2010. [Article \(CrossRef Link\)](#)
- [18] M. Matthaiou, N. D. Chatzidiamantis, G. K. Karagiannidis, and J. A. Nossek, "ZF Detector over Correlated K Fading MIMO Channels," *IEEE Trans. Commun.*, vol. 59, no. 6, pp. 1591-1603, Jun. 2011. [Article \(CrossRef Link\)](#)
- [19] K. Krishnamoorthy, *Handbook of Statistical Distributions with Application*. Chapman, Hall, 2006. [Article \(CrossRef Link\)](#)
- [20] M. K. Simon, and M. S. Alouini, "Digital Communication over Fading Channels: A Unified Approach to Performance Analysis," 2nd ed. John Wiley & Sons. Inr., 2005. [Article \(CrossRef Link\)](#)
- [21] I. S. Gradshteyn and I. M. Ryzhik, "Table of Integrals, Series, and Products, 7th ed. San Diego, CA: Academic Press, 2007.
- [22] A. W. Marshall and I. Olkin, "Inequalities: Theory of Majorization and Its Applications," *Springer-Verlag New York Inc.*, 2nd ed. 2011. [Article \(CrossRef Link\)](#)
- [23] D. P. Palomar, and Y. Jiang, "MIMO Transceiver Design via Majorizations," *Found. Trends Commun. Inf. Theory*, vol. 3, no. 4-5, pp. 331-551, 2006. [Article \(CrossRef Link\)](#)

- [24] E. Jorswieck and H. Boche, "Majorization and Matrix-Monotone Functions in Wireless Communications," *Found. Trends Commun. Inf. Theory*, vol. 3, no. 1567-2190, Jun. 2007. [Article \(CrossRef Link\)](#)
- [25] A. A. P. Guimaraes, and C. C. Cavalcante, "An Upper-Bound on the Ergodic Capacity of Rayleigh-Fading MIMO Channels Using Majorization Theory," *Simposio Brasileiro De Telecommun.*, pp. 13-16, Sep. 2012. [Article \(CrossRef Link\)](#)
- [26] C. Zhong, K.-K. Wong, and S. Jin, "Capacity bounds for MIMO Nakagami- m Fading Channels," *IEEE Trans. Signal Process.* vol. 57, no. 9, pp. 3613-3623, Sep. 2009. [Article \(CrossRef Link\)](#)
- [27] R. A. Horn and C. R. Johnson, "Matrix Analysis," *New York: Cambridge Press*, 1985. [Article \(CrossRef Link\)](#)
- [28] O. Oyman, R. U. Nabar, H. Bolcskei, and A. J. Paulraj, "Characterizing the Statistical Properties of Mutual Information in MIMO Channels," *IEEE Trans. Signal Process.*, vol. 51, no. 11, pp. 2784-2795, Nov. 2003. [Article \(CrossRef Link\)](#)
- [29] S. Verdú, "Spectral Efficiency in the Wideband Regime," *IEEE Trans. Inf. Theory*, vol. 48, no. 6, pp. 1319-1343, Jun. 2001. [Article \(CrossRef Link\)](#)
- [30] A. Lozano, A. M. Tulino, and S. Verdú, "Multiple-antenna Capacity in the Low-power Regime," *IEEE Trans. Inf. Theory*, vol. 49, no. 10, pp. 2527-2544, Oct. 2003. [Article \(CrossRef Link\)](#)
- [31] C. Zhong, S. Jin, K.-K. Wong, M.-S. Alouini, and T. Ratnarajah, "Low SNR Capacity for MIMO Rician and Rayleigh-Product Fading Channels with Single Co-Channel Interferer and Noise," *IEEE Trans. Commun.*, vol. 58, no. 9, pp. 2549-2560, Sep. 2010. [Article \(CrossRef Link\)](#)
- [32] L. Lu, G. Li, A. Swindlehurst, A. Ashikhmin, and R. Zhang, "An Overview of Massive MIMO: Benefits and Challenges," *IEEE J. Sel. Topics Signal Process.*, vol. 8, no. 5, pp. 742-758, Oct. 2014. [Article \(CrossRef Link\)](#)
- [33] M. Jo, D. Araujo, T. Maksymyuk, A. Almeida, and T. F. Maciel, "Massive MIMO: Survey and Future Research Topics," *IET Commun.*, pp.1-26, 2016. [Article \(CrossRef Link\)](#)
- [34] X. Li, L. Li, L. Xie, X. Su, and P. Zhang, "Performance Analysis of 3D Massive MIMO Cellular Systems with Collaborative Base Station," *Int. J. Antennas Propagat.*, vol. 2014, no. 614061, pp. 1-12, Jul. 2014. [Article \(CrossRef Link\)](#)
- [35] M. Abramowitz and I. A. Stegun, *Handbook of Mathematical Functions with Formulas, Graphs, and Mathematical Tables*, 9th ed. New York: Dover, 1972. [Article \(CrossRef Link\)](#)
- [36] The Wolfram | Alpha Site [Online]. Available: [Article \(CrossRef Link\)](#).
- [37] C. Kong, C. Zhong, M. Matthaiou, and Z. Zhang, "Performance of Downlink Massive MIMO in Rician Fading Channels with ZF Precoder," in *Proc. of IEEE Int. Conf. Commun. (ICC)*, pp. 1776-1782, 2015. [Article \(CrossRef Link\)](#)
- [38] A. Grant, "Rayleigh Fading Multi-Antenna Channels," *Eurasip J. Appl. Signal Process.*, vol. 2002, no. 3, pp. 316-329, Mar. 2002. [Article \(CrossRef Link\)](#)
- [39] A. P. Prudnikov, Y. A. Brychkov, and O. I. Marichev, *Integrals and Series, Volume 3, More Special Function*. New York: Gordon Breach, 1986. [Article \(CrossRef Link\)](#)



Xingwang Li received the B.Sc. degree in communication engineering from Henan Polytechnic University, China, in 2007. He then received the M. Sc. degree from the National Key Laboratory of Science and Technology on Communications at University of Electronic Science and Technology of China (UESTC) and Ph. D. degrees in communication and information system from the State Key Laboratory of Networking and Switching Technology at Beijing University of Posts and Telecommunications (BUPT). He is currently a lecturer with the College of Computer Science and Technology, Henan Polytechnic University, Jiaozuo China. His research interests include massive MIMO, hardware constrained communication, FSO communications, and performance analysis of fading channels. Email: lixingwangbupt@gmail.com.



Junfeng Wang received the B. Sc. And M. Sch. degrees in communication engineering from North University of China, Taiyuan, China in 2003 and 2007, respectively. He is current a lecturer with College of Computer Science and Technology, Henan Polytechnic University. His current research interests include signal and information processing, wireless communication. E-mail: wangjunfeng@hpu.edu.cn.



Lihua Li received her doctor degree in 2004 at Beijing University of Posts and Telecommunications (BUPT). She is currently an associate professor in BUPT. She had been a short -term visiting scholar at Brunel University in UK in 2006. And she visited the University of Oulu from August 2010 to August 2011. Her research focuses on wideband mobile communication technologies including MIMO, link adaptation, cooperative transmission technologies etc. relating to new generation mobile communication systems such as LTE and IMT - Advanced. She has published 63 papers in international and domestic journals and academic conferences, and 5 books. She has applied 20 national invention patents and one international patent. She was selected and funded as one of the New Century Excellent Talents by the Chinese Ministry of Education in 2008. She has won the second prize of China State Technological Invention Award (the 1st level award in China) in 2008 and the first prize of China Institute of Communications Science and Technology Award in 2006 for her research achievements of “Wideband Wireless Mobile TDD-OFDM -MIMO Technologies”. She has served as a group leader in 3GPP LTE RAN1 standardization work on behalf of BUPT in 2005, when she submitted more than 20 relevant proposals to 3GPP LTE and 7 of them were accepted. She has taken part in China IMT-Advanced technology work group since 2007. And so far she has submitted 33 relevant proposals, 15 of which were accepted. Email: lilihua@bupt.edu.cn.



Charles Casimiro Cavalcante received the B.Sc and M.Sc in Electrical Engineering from the Federal University of Cear (UFC), Brazil, in 1999 and 2001, respectively, and the Ph.D. degree from the University of Campinas (UNICAMP), Brazil, in 2004. He has held a grant for Scientific and Technological Development from 2004 to 2007 and since March 2009 he has a grant of Scientific Research Productivity both from the Brazilian Research Council (CNPq). From March 2007 to November 2008 he was a Visiting Professor at Teleinformatics Engineering Department of UFC and since November 2008 he is an Assistant Professor at the same department and university holding the Statistical Signal Processing chair. From August 2014 to July 2015 he was a Visiting Assistant Professor at the Department of Computer Science and Electrical Engineering (CSEE) from University of Maryland, Baltimore County (UMBC) in the United States. He has been working on signal processing strategies for communications where he has several papers published in journal and conferences, has authored three international patents and he has worked on several funded research projects on the signal processing and wireless communications areas. He is also a co-author of the book Unsupervised Signal Processing: Channel Equalization and Source Separation, published by CRC Press. He is a researcher of the Wireless Telecommunications Research Group (GTEL) where he leads research on signal processing and wireless communications. Dr. Cavalcante is a Senior Member of the IEEE and Senior Member of the Brazilian Telecommunications Society (SBrT). His main research interests are in signal processing for communications, blind source separation, wireless communications, and statistical signal processing